AD-A195 504 INVESTIGATION OF SUPERRADIANT LDV MARKERS AND THREE-COMPONENT VELOCITY MA..(U) YALE UNIV NEW HAVEN CT DEPT OF APPLIED PHYSICS R K CHANG ET AL. 10 MAR 88 1/1

UNCLASSIFIED AFOSR-TR-88-0641 F49620-85-K-0002 F/G 14/2 NL

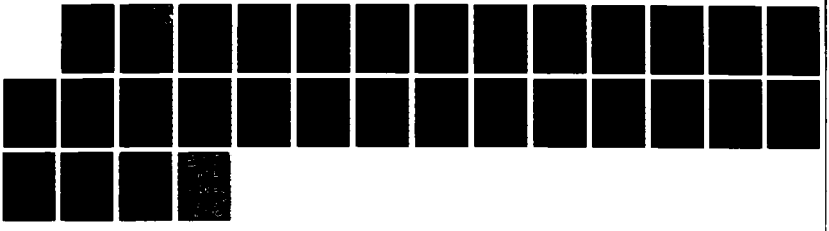

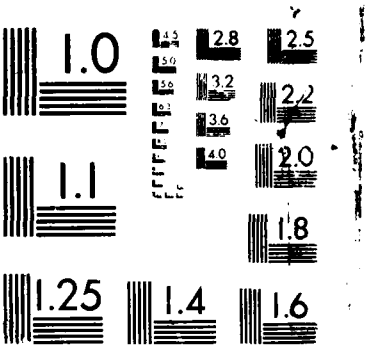

AD-A195 504

DOCUMENTATION PAGE

Form Approved OMB No. 0704-0188

1b. RESTRICTIVE MARKINGS

2a. SECURITY CLASSIFICATION AUTHORITY

3. DISTRIBUTION/AVAILABILITY OF REPORT
Approved for public release; distribution is unlimited.

2b. DECLASSIFICATION/DOWNGRADING SCHEDULE

4. PERFORMING ORGANIZATION REPORT NUMBER(S)

5. MONITORING ORGANIZATION REPORT NUMBER(S)
AFOSR-TR- 88-0641

6a. NAME OF PERFORMING ORGANIZATION
Yale University
Applied Physics

6b. OFFICE SYMBOL (If applicable)

7a. NAME OF MONITORING ORGANIZATION
AFOSR/NA

6c. ADDRESS (City, State, and ZIP Code)
New Haven, CT 06520

7b. ADDRESS (City, State, and ZIP Code)
Building 410, Bolling AFB DC 20332-6448

8a. NAME OF FUNDING/SPONSORING ORGANIZATION
AFOSR

8b. OFFICE SYMBOL (If applicable)
NA

9. PROCUREMENT INSTRUMENT IDENTIFICATION NUMBER
Contract No. F49620-85-K-0002

8c. ADDRESS (City, State, and ZIP Code)
Building 410, Bolling AFB DC 20332-6448

10. SOURCE OF FUNDING NUMBERS

PROGRAM ELEMENT NO.	PROJECT NO.	TASK NO.	WORK UNIT ACCESSION NO.
61102F	2308	A3	

11. TITLE (Include Security Classification)
(U) INVESTIGATION OF SUPERRADIANT LDV MARKERS AND THREE-COMPONENT VELOCITY MAPPING

12. PERSONAL AUTHOR(S)
Chang, Richard K., Long, Marshall B., and Kuc, Roman

13a. TYPE OF REPORT	13b. TIME COVERED	14. DATE OF REPORT (Year, Month, Day)	15. PAGE COUNT
FINAL	FROM 1/1/85 TO 12/31/87	1988 March 10	25

16. SUPPLEMENTARY NOTATION

17. COSATI CODES		
FIELD	GROUP	SUB-GROUP

18. SUBJECT TERMS (Continue on reverse if necessary and identify by block number)
Liquid droplets
Plasma spectroscopy
Nonlinear optical effects
Laser-induced breakdown
Morphology-dependent resonances
Three-dimensional scalar mapping
Three-dimensional velocity mapping
Multiple exposure holograms

19. ABSTRACT (Continue on reverse if necessary and identify by block number)

A summary is presented of our research progress in three areas: (1) micrometer-size droplets; (2) three-dimensional scalar mapping; and (3) three-dimensional velocity mapping.

Nonlinear optical interactions in a droplet occur at remarkably low input intensity levels because the droplet acts as a lens to concentrate the input radiation at a location just within the shadow face and as an optical cavity to provide feedback for the internally generated radiation. The following nonlinear optical effects have been observed in single droplets: (1) lasing; (2) stimulated Raman scattering up to the 14th order; (3) coherent Raman gain due to the presence of another input wave; (4) phase-modulation broadening of the elastically scattered and stimulated Raman scattered radiation; (5) the delay time in generating the multiorder stimulated Raman scattering; and

(Continued)

20. DISTRIBUTION/AVAILABILITY OF ABSTRACT
☒ UNCLASSIFIED/UNLIMITED ☒ SAME AS RPT ☐ DTIC USERS

21. ABSTRACT SECURITY CLASSIFICATION
Unclassified

22a. NAME OF RESPONSIBLE INDIVIDUAL
Julian M Tishkoff

22b. TELEPHONE (Include Area Code)
(202) 767-0465

22c. OFFICE SYMBOL
AFOSR/NA

DD Form 1473, JUN 86 Previous editions are obsolete. SECURITY CLASSIFICATION OF THIS PAGE

Unclassified

19. ABSTRACT (Continued):

(6) the effective Q-factor of the droplet cavity based on a lifetime measurement of the radiation trapped within the droplet.

Laser-induced breakdown (LIB) within the droplet occurs when the rising portion of the input laser pulse causes multiphoton ionization, which is followed by cascade multiplication. The resultant plasma within the droplet transforms a nominally transparent droplet into an absorping droplet, and the remaining portion of the input laser pulse heats the droplet. Plasma is ejected from the droplet, first from the shadow face and then from the illuminated face. Once the plasma has been quenched, the droplet undergoes explosive vaporization. We have measured the following properties of LIB and explosive vaporization: (1) the location of LIB initiation; (2) the propagation velocities of the ejected plasma; (3) the time-averaged electron density along a line; (4) the time-averaged atomic temperature along a line; and (5) the shape of the droplet undergoing explosive vaporization.

Three-dimensional scalar mapping was made possible by sweeping the laser illumination sheet and by recording scattered images on a high-speed framing camera. Such digitally recorded two-dimensional images from many sheets, all recorded in a time short compared to fluid motion, enabled us to construct iso-concentration surfaces in three dimensions. Three-dimensional scalar mapping measurements were made from aerosol-laden cold flows (via elastic scattering) and turbulent flames (via molecular specific fluorescence and Rayleigh scattering).

Three-dimensional velocity mapping was achieved by using a multiple-pulse holographic technique. The turbulent flow was seeded with many microballoons that were coated with silver to increase the elastic scattering. An in-line holography configuration was determined to produce the clearest holographic images on a high resolution sensitive film. In order to determine the direction and velocity of the seeded particles in the flow field, the illuminating beams were temporally coded. A digital image analysis technique was used to determine the direction and velocity magnitude of the flow within a three-dimensional sample volume.

FINAL REPORT

to the

Air Force Office of Scientific Research

INVESTIGATION OF SUPERRADIANT LDV MARKERS AND THREE-COMPONENT VELOCITY MAPPING

AFOSR Contract No. F49620-85-K-0002

January 1, 1985 - December 31, 1987

Richard K. Chang, Marshall B. Long, and Roman Kuc

Principal Investigators

Yale University

New Haven, Connecticut 06520

March 10, 1988

CONTENTS

INTRODUCTION

During the three years of AFOSR support, significant progress has been made in the following research areas:

Micrometer-Size Droplets. We have investigated high energy and high intensity laser beam interactions with single liquid droplets with radius, a, much larger than the incident laser wavelength, λ_o, i.e., droplets with large size parameters $X = 2\pi a/\lambda_o$. Our efforts involved nonlinear optical effects, such as lasing and four-wave mixing processes, and laser-induced breakdown (LIB) and explosive vaporization effects that occur during and after a laser pulse.

Three-Dimensional Scalar Mapping. We have developed diagnostic techniques that can illuminate the sample volume by a series of rapidly scanned thin sheets and can record data from many points on each sheet during a time short compared to the flow time scales.

Three-Dimensional Velocity Mapping. Our preliminary results on three-dimensional velocity mapping in aerosol seeded turbulent flows were achieved by developing a multiple-pulse volume hologram technique that uses silver coated glass balloons as markers and an image processing formalism to specify the locations of each marker in the reconstructed images.

RESEARCH ACCOMPLISHMENTS

A brief summary of our results in each of these research areas follows. Specific details of our accomplishments regarding droplets and scalar mapping can be found in the publications resulting from the research (see list on page 16). All these papers have been submitted to AFOSR in both preprint and reprint form.

MICROMETER-SIZE DROPLETS

The intent of this phase of the research was to develop laser diagnostic techniques applicable for two-phase flow. The first objective was to study bright wavelength-shifted markers that can be used to trace out the flow fields and be spectrally isolated from the unadvoidable elastic scattering from the container walls and turbulent medium. The second objective was to investigate nonlinear spectroscopic approaches that can identify the species within the droplet (as opposed to the gas surrounding the droplets). While we were pursuing these two objectives, several unexpected topics related to nonlinear optical effects in droplets warranted investigation by us.

Nonlinear Optical Effects in Droplets

When a plane wave is incident on a droplet with a large X, the droplet can be *envisioned* as a lens that concentrates the radiation in three places: (1) outside the shadow face, (2) just inside the shadow face, and (3) just inside the illuminated face. While these three locations can be qualitatively predicted by geometric optics, the exact amount of intensity enhancement in the locations requires detailed Lorenz-Mie calculations. Complete knowledge of these high intensity regions is important to all nonlinear optical and LIB studies. Our collaboration with Prof. Peter W. Barber's group at Clarkson University resulted in computer-intensive calculations of the internal- and near-field intensity distribution of a large X sphere and in an experimental mapping of these three locations of intensity concentration by a fluorescence technique. See publication # 1.

Another unique feature of a large X droplet is that its spherical liquid-air interface is capable of trapping some of the internally generated radiation (e.g., fluorescence or spontaneous Raman) when the wavelength is equal to one of the numerous wavelengths which correspond to morphology-dependent resonances (MDR's). With geometrics optics, it is known that internal rays which strike the liquid-air interface with angles larger

than the critical angle experience quasi-total internal reflection. Using a physical optics description, those internal rays which maintain the same phase front after completing one trip around the entire droplet circumference are trapped within the spherical interface. The droplet for specific wavelengths acts as an optical cavity to provide feedback for the internally generated radiation. Because of the optical feedback, lasing and stimulated Raman scattering (SRS) have been observed from liquid droplets with astonishingly low pump intensity thresholds. Color photographs show that the radiation of lasing droplets and of droplets undergoing SRS is confined just inside the liquid-air interface where the optical feedback is high. See publications #2 and #3 for color photographs.

The lasing spectra were noted to consist of sharp peaks within the broad fluorescence wavelength region. These lasing peaks are separated by nearly equal wavelengths, in accordance with the MDR's of a sphere with large X and with the index of refraction $m > 1$. Small changes in the lasing peaks have been used as indicators of small radius changes resulting from the evaporation of each droplet within the linear stream of flowing droplets. In addition, utilizing the small amount of wavelength oscillation in these peaks, we have deduced the amount of small shape oscillation. From the frequency and the damping rate of the oscillation amplitudes, we can extract the dynamic surface tension and the bulk viscosity of the droplet. See publication #4 for a summary of this diagnostic technique.

The SRS spectra can be used to provide information on the molecular species contained within the droplet and, to a lesser extent, information on the species concentration. The energy loss indicated by the wavelength of the SRS peaks (usually measured in wave number shifts from the input laser radiation) is equal to the molecular vibrational energy. Thus, the wave number locations of the SRS peaks are fingerprints of the molecular species contained within the droplet. The intensity of the SRS peaks has been shown to monotonically increase with species concentration. However, fluctuations in the SRS

peak intensity are large and, therefore, the SRS intensity is not an accurate measure of species concentration. For more details on the use of SRS for species identification, see publication #5.

In addition to lasing and SRS, three additional nonlinear optical effects were observed in large X and transparent droplets. One such nonlinear effect is multiorder Raman scattering which can be readily seen from liquid droplets. The second-order SRS can be pumped by the internal fields of the incident radiation and the first-order SRS. The third-order SRS can be pumped by the internal field of the second-order SRS. With such successive pumping by the first-order SRS process, up to the 14th-order SRS has been observed. See publication #6.

The second nonlinear optical effect observed from large X and transparent droplets is phase-modulation broadening of the elastically scattered radiation and of the SRS. Because the internal radiation at λ_0 and at the multiorder SRS wavelengths is so intense, the refractive index of the droplet is altered, i.e., m changes from m_0 at low intensity to $m_0 + n_2 I(t)$ at high intensity, where n_2 is commonly referred to as the intensity-dependent index of refraction. Since the refractive index is proportional to the time-varying intensity I(t), the internal waves circumventing the droplet-air interface experience a time-varying phase shift and, hence, a frequency modulation. Using a time-averaged detection system, the effect of frequency modulation is observed as a wavelength broadening of the scattered radiation originally centered at λ_0 and/or at the various multiorder SRS wavelengths. See publication #7.

Coherent Raman gain is the third nonlinear optical effect observed from large X and transparent droplets which are irradiated by two input beams with wavelengths at λ_0 and λ_1. The second beam provides additional Raman gain and parametric signals at the first-order Stokes of the first beam. The combined effect of the additional gain and the parametric signals due to the presence of the second beam is to lower the SRS threshold of the first beam. See publication #8.

Our research capabilities during the last year were greatly improved by the acquisition of several items of capital equipment. In particular, a streak camera enabled us to determine the time delay in building up the SRS in single droplets and the decay time of the SRS radiation trapped within the droplet. The first-order SRS build up time is between 5 and 7 nsec for Q-switched Nd:YAG laser pulses (λ_0 = 0.532 μm, 6 nsec pulse duration) and is ≈150 psec for mode-locked Q-switched Nd:YAG laser pulses (λ_0 = 0.532 μm, 100 psec pulse duration). The build up time of multiorder SRS is much shorter than that of first-order SRS. We have ascribed this to the fact that second-order SRS does not necessarily start from spontaneous Raman noise but can start from the parametric signal created by the laser and the first-order SRS. Furthermore, the gain experienced by the second-order SRS is more than that for the first-order SRS because of the additional Raman gain provided by the coherent Raman mixing effect. (See publication #9.) The decay time of the SRS trapped within the droplet depends on the Q-factor of the MDR's of the droplet, which acts as an optical cavity to provide the feedback for the internally generated Raman radiation. The SRS decay time is noted to arise from two factors: (1) the leakage of the SRS out of the droplet, commensurate with the Q-factor of the MDR's that can be calculated from the Lorenz-Mie theory for a perfect sphere, and (2) the intensity depletion of the SRS, resulting from the partial nonlinear optical conversion of the first-order SRS photons to second-order SRS photons, which, in turn, are partially converted to third-order SRS photons. By measuring the decay time of the SRS photons, the effective Q-factor of the droplet cavity was deduced. See publication #10.

Several invitations to international conferences on nonlinear optics gave us the opportunity to review our findings on optical effects from single droplets. See publications #11 - #14.

Laser-Induced Breakdown (LIB)

In laser diagnostics of droplets in a two-phase flow, the upper limit of the

laser intensity that can be sent into a sample chamber is set by the LIB threshold. The presence of fuel droplets greatly reduces the upper limit of the laser inensity as a result of the focusing effect of each droplet and the lower breakdown threshold of some liquids relative to the surrounding gas. For this reason, we decided to investigate the LIB characteristics of transparent droplets with large X.

Ethanol droplets containing efficient fluorescent molecules are known to reach the laser threshold at remarkably low input pump intensity. We therefore investigated the emission properties of lasing droplets at input pump intensity levels far beyond the lasing thresholds. The following sequence of emission events occurs as a function of increasing pump intensity: (1) lasing emission is reached with low input intensity; (2) both SRS and laser emission are noted at higher input intensity; (3) the internal laser intensity is sufficient to induce SRS at still higher input intensity; and (4) the LIB threshold is reached when the input pump intensity reaches ≈ 1 GW/cm^2, causing the appearance of an intense continuum emission associated with the recombination of the plasma and the deceleration of the electrons. Once the LIB threshold has been reached, the plasma emission is observed from not only within the droplet but also outside it in the region behind the illuminated face. Whereas the emission within the droplet consists of a broad continuum that extends toward the UV range, the emission outside the droplet consists of a broad continuum and discrete peak emission, which is characteristic of fluorescence from highly excited atomic and ionized species, such as singly ionized nitrogen N(II) and singly ionized oxygen O(II) in air. For more details, see publication #15.

One of the key questions in the field of the LIB of transparent droplets with $X >> 1$ is the location of the breakdown initiation, i.e., is the breakdown initiated within the droplet shadow face where the internal intensity is concentrated or outside the droplet shadow face where the external intensity is even higher than the internal intensity? We modified our spectrograph in such a way that the spatial information along the vertical

spectrograph slit is preserved. If a two-dimensional optical multichannel vidicon is placed at the exit plane of the spectrograph, this vidicon can detect both the spectral information dispersed along the horizontal direction and the spatial information preserved along the vertical direction. This instrument then enables us to determine simultaneously the plasma emission from many points (both within and outside the droplet) along an axis parallel to the laser beam. Our results indicate that LIB is initiated outside the shadow face for water droplets surrounded by a low LIB threshold gas such as Ar. However, LIB is initiated inside the shadow face for water droplets (radius < 40 μm) surrounded by air. In the case of larger water droplets (radius > 50 μm) surrounded by air, the location of LIB initiation shifts to the region outside the shadow face. For fluorocarbon (C_8F_{18}) liquid, known for its high dielectric breakdown strength, the LIB of C_8F_{18} droplets is always initiated in the gas region outside the droplet shadow face. For more details, see publications # 16 and # 17.

Another key question in field of the LIB of transparent droplets relates to the electron density and species temperature within different parts of the plasma plumes that are ejected from the droplet interface. We used the spatial preserving spectrograph-vidicon instrument described above to determine the plasma emission line shape along a line parallel to the laser beam. The spectral linewidth of discrete emission peaks from atomic species is known to be broadened by the electric fields of the electrons surrounding the atomic species, i.e., atomic line broadening results from the electric fields of the electrons through the first- or second-order Stark effect. We were, therefore, able to extract the spatial variation of the electron density along a line by noting the linewidth broadening of the atomic emission peak along a line that encompasses the regions outside the droplet illuminated and shadow faces. In addition to a density variation, an asymmetry in the electron density is noted in these two regions. Based on the appearance of a line reversal in the line shape of the resonance emission from Na or Li markers placed in the water droplet in the form of NaCl or LiCl, we conclude that the

region in front of the shadow face is optically thicker than the region behind the illuminated face. The intensity ratio of two discrete wavelength peaks of the same species can be used as an indicator of the species temperature, provided that local thermodynamic equilibrium has been reached within the plasma plume. We measured the intensity ratio of the hydrogen Balmer lines and were able to extract the hydrogen temperature along a line which encompasses the regions outside the droplet illuminated and shadow faces. See publication # 18.

The spectroscopic instrument used to determine the location of the LIB initiation, the electron density, and the atomic species temperature had spatial resolution but lacked temporal resolution. A streak camera that has a time resolution in the 0.1 nsec range was used to measure the propagation velocity of the plasma emission front by imaging a line, which encompasses the region within the droplet and the regions outside the droplet illuminated and shadow faces, on the vertical slit of the streak camera. Using this technique, we also determined the propagation velocity of the plasma emission for the following: (1) the plasma ejected from the droplet shadow face; (2) the plasma traveling inside the droplet from the shadow face toward the illuminated face; (3) with the laser pulse on, the plasma ejected from the illuminated face after the internal plasma has reached the illuminated face; and (4) with the laser pulse off, the external plasma traveling toward the laser from the droplet illuminated face. At high input intensites, the propagation velocities of the plasma traveling toward the laser provide information on the optical detonation wave. The response of our streak camera is not fast enough for us to determine the velocity of the breakdown wave that is initiated just outside the droplet shadow face during the rising portion of the laser pulse. See publication # 19.

A transparent droplet is transformed into an absorbing droplet once LIB occurs. The plasma produced by the LIB process during the initial part of the laser pulse can absorb and scatter the remaining part of the incident radiation. Once LIB is initiated within the

droplet shadow face region, the absorbed laser energy is subsequently localized in this region. This localized absorption eventually heats the entire droplet via the thermal diffusive mechanism which takes several milliseconds for micrometer-size droplets. A framing camera enabled us to photograph a droplet every 50 nsec with a frame time of 10 nsec. Using a back-illuminated technique, we photographed a transparent water droplet at various time delays after irradiation by a green high intensity laser beam (λ_0 = 0.532 μm). Such ultrafast photographs reveal that vapor first emerges from the droplet shadow face and that the shadow face is partially consumed by the vaporization process. At a subsequent time, long after the laser pulse is shut off, more and more of the droplet shadow face is consumed as the heat travels from the shadow face toward the illuminated face. We were able to measure the ejected vapor velocity, the receding velocity of the liquid-air interface starting from the shadow face side, and the velocity of the remaining droplet as it is propelled toward the laser by the rapid vaporization occurring at the shadow face after LIB has been initiated. See publication #20.

A request to contribute a paper for a special issue of Applied Optics devoted to propagation and scattering in the atmosphere gave us a chance to review our work in the field of LIB in transparent liquid droplets. See publication #21.

Detector Improvement

During the previous AFOSR contract period, we needed to increase the sensitivity of the silicon intensified target (SIT) vidicon camera. A summary of our results on the coupling of an electrostatic image-intensifier on one end and a SIT vidicon on the other end of a coherent fiber-optics bundle can be found in publication #22. The image-intensifier raised the lower detectivity limit of the standard SIT vidicon.

THREE-DIMENSIONAL SCALAR MAPPING

Turbulent flow is inherently three-dimensional and, although two-dimensional measurements have provided valuable insight into important large-scale flow phenomena, ambiguities remain. Work has been done to extend two-dimensional scalar mapping techniques into the third dimension. To solve the general problem of three-dimensional measurements in turbulent flow, data must be recorded from many points within a volume in times on the order of 10 μsec (as dictated by the flow time scales). This requirement places high demands on both the laser source and the data acquisition system used for the measurement. During the research period, progress has been made, however, and instantaneous three-dimensional measurements in turbulent flames have now been demonstrated.

In early phases of the work on the extension of laser imaging techniques from two to three dimensions, several different approaches were pursued. One of the easiest means of assembling three-dimensional information on flow structures is to investigate an externally forced repeatable flow. By performing measurements at a constant time delay after the introduction of a perturbation, a series of two-dimensional measurements taken at different times can be assembled into a three-dimensional data set. This approach is desirable since it removes the requirement of very high-speed data acquisition and allows signals from relatively weak scattering mechanisms to be accumulated. From the standpoint of fluids, however, there is no doubt that the structures in forced flows do not adequately represent the characteristics of fully developed turbulent flow.

For this reason, a continued effort was made to develop techniques for very high-speed imaging of multiple illumination sheets. In one experiment, a series of parallel sheets was produced by rapidly scanning a thin illumination sheet produced by a cavity-dumped Ar^+ laser through an aerosol seeded jet. The image of the Lorenz-Mie scattering from the aerosols was directed onto different regions of a doubly intensified vidicon

detector by a rotating mirror. Since the duration of pulses from the cavity dumped Ar^+ laser was only 10 nsec, no blurring of the images occurred as a result of the rotation of the mirrors. With this approach, it was possible to achieve an effective framing rate of 30 kHz, thus allowing six different flow planes to be recorded in 200 μsec.

The experiment was subsequently improved by replacing the rotating mirror in front of the detector with a high-speed electronic framing camera. With this modification, a framing rate of 100 kHz was possible, allowing us to record 16 frames corresponding to 16 different locations of the sweeping illumination sheet. With our new detector, the main limitation now had to do with the relatively low power of the laser source. Using an Ar^+ laser, the laser energy in each exposure time was <1 μJ. Thus, Lorenz-Mie scattering was the only viable scattering mechanism that could be used. A complete discussion of this preliminary work can be found in publications #23 and #24.

In our most recent work, we have succeeded in performing a truly instantaneous three-dimensional measurement in a turbulent flame by detecting molecular scattering. The experiments were done at the Combustion Research Facility at Sandia National Laboratories using a flashlamp pumped dye laser as the illumination source. By using this laser in conjunction with the high-speed electronic framing camera, it was possible to record the fluorescence from 12 parallel light sheets intersecting a volume of the flow during a single 1 μsec laser pulse. Because of the high average power during the relatively long 1 μsec pulse, molecular scattering could be detected. The framing camera was used in its highest framing rate mode of 2×10^7 frames/sec. This work is described in publication #25.

THREE-DIMENSIONAL VELOCITY MEASUREMENT

Because it is the velocity that enters directly into the equations of motion for fluid flow, its measurement is of critical importance. For this reason, the use of multiple-pulse holography to provide velocity information at a large number of points within a

volume was also investigated. In this work, a hologram of an aerosol seeded flow was recorded on film for later digital analysis. To provide optimum scattering from the tagging particles, aphenolic microballoons were coated with a thin layer of silver. This allowed sufficient scattering to adequately expose the high resolution, low sensitivity film used to record the hologram. Following the development of the hologram, the real image was reconstructed in a series of planes digitized using the high resolution scanning diode array camera. Algorithms for efficient processing of the large data set obtained from the digitized real images were also developed. Some details of this work are given in the following sections.

Hologram Generation

The two most commonly used holographic methods differ primarily in their means of reference beam generation. For in-line holography, a single beam is used as both the reference and object beam. Off-axis holography uses two separate beams with the reference beam and the scattered object beam being combined at the recording medium. Both approaches were investigated. In-line holography was found to provide the best results because of its relative simplicity, moderate film resolution requirements, and the efficiency of forward scattering from the aerosol particles used to tag the flow.

Although the feasibility of double-pulse holography for determining velocity has previously been demonstrated, the method has not gained widespread acceptance. This is due in part to the lack of an automated data analysis process to extract velocity data from the reconstructed image pairs. One of the problems in the analysis is the difficulty in determining which images correspond to a given particle. In addition, there can be ambiguity in determining the direction of the flow. Both of these problems can be made more tractable by using a large number of temporally coded pulses to form the hologram. The larger amount of information included in the hologram can be used in the analysis

phase to resolve the image matching and directional ambiguities that limit the success of the double-pulse technique.

To form the multiple-pulse hologram, an argon-ion laser beam was modulated to form a series of illumination pulses of the desired pulse duration and separation. The modulation was produced by two acousto-optic modulators that were controlled by a pulse forming circuit. The duration of each pulse was selected so that the particles in the flow would not move more than 1/10 of their diameter during the pulse. The separation between pulses was varied to remove directional ambiguity, and both the pulse duration and separation could be adjusted to suit the flow conditions. For our experiments, a series of five pulses was used. The pulse duration was 8 μsec and the total measurement time (i.e., the time between the first and fifth pulse) was 500 μsec. The laser beam was spatially filtered to provide a smooth intensity profile and then passed through an air jet seeded with aerosols. The photographic film that recorded the hologram was located 300 mm from the jet, ensuring that the far-field requirement of in-line holography was satisfied.

The aerosols consisted of silver-coated aphenolic resin microballoons. Chemically coating the particles with a thin layer of silver significantly improved the image contrast and resulted in clear, bright images. The increase in contrast obtained by chemically coating the microballoons was observed experimentally and also confirmed by a layered sphere calculation. The microballoons had a density of 0.072 g/cm^3 and a diameter range of 5 - 124 μm. A 90 mm-diameter hologram of the aerosol was recorded on Kodak technical film 2415, which provided adequate resolution (320 line pairs/mm) and sensitivity (0.2 ergs/cm^2) for the in-line hologram.

Hologram Reconstruction

The optical setup for the reconstruction process was similar to the setup used in the formation of the hologram, except for the absence of the seeded jet and the addition

of a 600 mm focal length lens to collimate the beam. The collimated beam illuminated the hologram and produced a real image of the multiply exposed aerosol particles. Spatial filtering was used to remove most of the undiffracted beam so that a high contrast image of the aerosol could be produced. A lens that focused the undiffracted portion of the beam to a point at the lens' focal plane was placed behind the hologram in order to accomplish the high-pass spatial filtering. This undiffracted portion was blocked by an opaque spot on a microscope slide. The diffracted light from the hologram formed a real image of the aerosol further from the spatial filtering lens. The real image of the aerosols fell directly onto a high resolution photodiode array camera. Different planes of the image were brought into focus by moving the hologram (mounted on a stepping motor driven stage) toward or away from the spatial filtering lens.

Image Analysis and Velocity Determination

There are three steps in the procedure to map the three-dimensional velocity field using the multiple-pulse hologram of the seeded flow. First, the location of each aerosol image in the hologram must be accurately determined. Second, the seed images must be grouped into a set that was generated by a particular seed object. Finally, the velocity magnitude and direction must be determined for each group. There are several physical constraints on the images that can be exploited to make this complex problem more tenable.

The location of each image must be determined in the first phase of the analysis. The data contained in the hologram are recorded by focusing a set of two-dimensional planes of the hologram onto a high-resolution camera and digitizing the resulting images. Two components (x and y) of a particle image location can be obtained by computing the centroid of an iso-intensity contour. If the optics used to reconstruct the hologram are selected so that the depth of focus of the real image is small, an accurate measurement of the z location can be made by determing the location of the best focus of the point

image. The best focus can be determined by considering both the maximum intensity and minimum image dimension of the particle. Upon completion of this process, a list of all the image positions and intensities will be recorded in an array.

The next step in the image analysis of the hologram is to group the images into sets that can be assigned to the same aerosol particle (5 images/particle were used for our experiment). As a first step, the problem can be simplified by using our knowledge of the laser pulsing pattern and the maximum expected velocity in the flow. With this information, a reduced volume can be determined within which all of the images corresponding to a single particle must reside. The list of all image locations can be searched and those falling outside this volume can be excluded. If the aerosol seeding density is low, there may be only 5 particle images in this volume and the grouping will be complete. If more than 5 images lie within this volume, an additional search can be performed to determine which images most closely lie along a straight line and satisfy the constraints imposed by the temporal coding of the light pulses. As groups of images are found, they are eliminated from the original table to make subsequent searches more efficient.

Once the first two steps are complete, it is relatively straightforward to determine the magnitude, orientation, and direction of the velocity. The orientation can be determined from a least squared straight line fit through the points in three dimensions. The direction is determined from the irregular spacing of the images (corresponding to the temporal coding of the light pulses) and the magnitude from the distance between extreme points.

PUBLICATIONS RESULTING FROM THE RESEARCH

MICROMETER-SIZE DROPLETS

Nonlinear Optical Effects

1. D. S. Benincasa, P. W. Barber, J.-Z. Zhang, W.-F. Hsieh, and R. K. Chang, "Spatial Distribution of the Internal and Near-Field Intensities of Large Cylindrical and Spherical Scatterers," Appl. Opt. 26, 1348 (1987).

2. S.-X. Qian, J. B. Snow, H.-M. Tzeng, and R. K. Chang, "Lasing Droplets: Highlighting the Liquid-Air Interface by Laser Emission," Science 231, 486 (1986).

3. J. B. Snow, S.-X. Qian, and R. K. Chang, "Nonlinear Optics with a Micrometer-Size Droplet," Opt. News 12 (5), 5 (1986).

4. H.-M. Tzeng, M. B. Long, R. K. Chang, and P. W. Barber, "Size and Shape Variations of Liquid Droplets Deduced from Morphology-Dependent Resonances in Fluorescence Spectra," in Proceedings of the SPIE Particle Sizing and Spray Analysis Conference, Vol. 573 (SPIE, Bellingham, Washington, 1985), p. 80.

5. J. H. Eickmans and R. K. Chang, "Stimulated Raman Scattering Spectra from Single Water Droplets," in Proceedings of the Tenth International Conference on Raman Spectroscopy, W. L. Peticolas and B. Hudson, eds. (University of Oregon, Eugene, 1986), p. 8-7.

6. S.-X. Qian and R. K. Chang, "Multiorder Stokes Emission from Micrometer-Size Droplets," Phys. Rev. Lett. 56, 926 (1986).

7. S.-X. Qian and R. K. Chang, "Phase-Modulation-Broadened Line Shapes from Micrometer-Size CS_2 Droplets," Opt. Lett. 11, 371 (1986).

8. S.-X. Qian, J. B. Snow, and R. K. Chang, "Coherent Raman Mixing and Coherent Anti-Stokes Raman Scattering from Individual Micrometer-Size Droplets," Opt. Lett. 10, 499 (1985).

9. W.-F. Hsieh, J.-B. Zheng, and R. K. Chang, "Time Dependence of Multiorder Stimulated Raman Scattering from Single Droplets," submitted to Opt. Lett.

10. J.-Z. Zhang, D. H. Leach, and R. K. Chang, "Photon Lifetime within a Droplet: Temporal Determination of Elastic and Stimulated Raman Scattering," Opt. Lett., in press.

11. R. K. Chang, S.-X. Qian, and J. Eickmans, "Stimulated Raman Scattering, Phase Modulation, and Coherent Anti-Stokes Raman Scattering from Single Micrometer-Size Liquid Droplets," in Methods of Laser Spectroscopy, Y. Prior, A. Ben-Reuven, and M. Rosenbluh, eds. (Plenum Press, New York, 1986), p. 249.

12. R. K. Chang, "Micrometer-Size Droplets as Optical Cavities: Lasing and Other Nonlinear Effects," in Advances in Laser Science-II, M. Lapp, W.C. Stwalley, and G.A. Kenney-Wallace, eds. (American Institute of Physics, New York, 1987), p. 509.

13. R. K. Chang, D. H. Leach, and J.-Z. Zhang, "The Q-Factor of Micrometer-Size Droplets as Optical Cavities," to be published in the Proceedings of the U.S.-Mexico Workshop on Electrodynamics of Interfaces and Composite Systems, Taxco, Mexico, August 10-14, 1987.

14. R. K. Chang, "Nonlinear Optical Phenomena in Single Micron-Size Droplets," in Laser Optics of Condensed Matter, J. L. Birman, H. Z. Cummins, and A. A. Kaplyanski, eds. (Plenum Press, New York), in press.

Laser-Induced Breakdown (LIB)

15. W.-F. Hsieh, H.-M. Tzeng, and R. K. Chang, "High Intensity Laser Interactions with Micrometer-Size Dye Droplets," in Special Issue of the Annual Report of the Institute of Physics, Academia Sinica (Taiwan), Vol. 16, 1986, p. 1.

16. J. H. Eickmans, W.-F. Hsieh, and R. K. Chang, "Laser-Induced Explosion of H_2O Droplets: Spatially Resolved Spectra," Opt. Lett. 12, 22 (1987).

17. W.-F. Hsieh, J. H. Eickmans, and R. K. Chang, "Internal and External Laser-Induced Avalanche Breakdown of Single Droplets in an Argon Atmosphere," J. Opt. Soc. Am. B 4, 1816 (1987).

18. J. H. Eickmans, W.-F. Hsieh, and R. K. Chang, "Plasma Spectroscopy of H, Li, and Na in Plumes Resulting from Laser-Induced Droplet Explosion" Appl. Opt. 26, 3721 (1987).

19. W.-F. Hsieh, J.-B. Zheng, C. F. Wood, B. T. Chu, and R. K. Chang, "Propagation Velocities of Laser-Induced Plasma inside and outside a Transparent Droplet," Opt. Lett. 12, 576 (1987).

20. J.-Z. Zhang, J. K. Lam, C. F. Wood, B. T. Chu, and R. K. Chang, "Explosive Vaporization of a Large Transparent Droplet Irradiated by a High Intensity Laser," Appl. Opt. 26, 4731 (1987).

21. R. K. Chang, J. Eickmans, W.-F. Hsieh, C. F. Wood, J.-Z. Zhang, and J.-B. Zheng, "Laser-Induced Breakdown in Large Transparent Water Droplets," Appl. Opt., in press.

Detector Improvement

22. J. B. Snow, J.-B. Zheng, and R. K. Chang, "Increased Sensitivity of a Vidicon Optical Multichannel Analyzer with a Detachable Electrostatic Image Intensifier," Appl. Opt. 25, 172 (1986).

THREE-DIMENSIONAL SCALAR MAPPING

23. B. Yip and M. B. Long, "Three-Dimensional Measurements in Gas Flows," in Proceedings of the Fifth Internaitonal Congress on Applications of Lasers and Electro-Optics. Vol. 58 (Laser Institute of America, Toledo, Ohio, 1987), p. 1.

24. B. Yip, J. K. Lam, M. Winter, and M. B. Long, "Time-Resolved Three-Dimensional Concentration Measurements in a Gas Jet," Science 235, 1209 (1987).

25. B. Yip, R. L. Schmitt, and M. B. Long, "Instantaneous Three-Dimensional Concentration Measurements in Turbulent Jets and Flames," Opt. Lett. 13, 96 (1988).

SCIENTIFIC COLLABORATORS

In addition to the Co-Principal Investigators, the following people have participated in this project:

Theorists:	Peter W. Barber, Clarkson University
	Stephen C. Hill, Clarkson University
	Boa-Teh Chu, Yale University
Postdoctoral Associates:	Carol Wood
	Viroj Vilimpac
Graduate Students:	David Leach
	Jian-Zhi Zhang

LECTURES PRESENTED ABOUT THE RESEARCH

Richard K. Chang:

"Linear and Nonlinear Optical Effects from Microparticles," AT&T Research Laboratories, Holmdel, NJ, 5/30/85.

"Laser Emission and Stimulated Raman Scattering from Liquid Droplets," 1985 CRDC Scientific Conference on Obscuration and Aerosol Research, Aberdeen Proving Ground, MD, 6/19/85.

"Light Scattering from a Fiber Placed near a Mirror: Case Study of Multiple Scattering," 1985 CRDC Scientific Conference on Obscuration and Aerosol Research, Aberdeen Proving Ground, MD, 6/21/85.

"Linear and Nonlinear Optical Scattering from Micron Size Droplets," 5th International Conference on Surface and Colloid Science, Potsdam, NY, 6/25/85 (invited talk).

"Nonlinear Optical Spectroscopy of Single Liquid Droplets," Gordon Conference on the Physics and Chemistry of Laser Diagnostics in Combustion, New London, NH, 7/29/85 (invited talk).

"Morphology-Dependent Resonances and Their Effect on Laser Scattering from Droplets," Standard Oil Company, Cleveland, OH, 7/24/85.

"Nonlinear Optical Spectroscopy of Single Liquid Droplets," Air Force Office of Scientific Research Colloquium, Bolling Air Force Base, Washington, DC, 8/14/85.

"Stimulated Emissions from Micrometer-Size Droplets," Physics Department, City College, CUNY, New York, NY, 9/4/85.

"Linear and Nonlinear Optical Effects on Micron-Size Particles," Electrical Engineering Department, SUNY, Buffalo, NY, 10/4/85.

"Lasing and Nonlinear Optical Scattering from Individual Liquid Droplets," Annual Meeting of the Optical Society of America, Washington, DC, 10/17/85 (invited talk).

"Nonlinear Optical Emission from Single Liquid Droplets," Fritz-Haber Institute Symposium on Methods of Laser Spectroscopy, Weizmann Institute of Science, Rehovot, Israel, 12/15/85 (invited talk).

"Nonlinear Optical Effects in Liquid Droplets: Results from High Intensity Lasers," Workshop on the Interactions of Electromagnetc and Particle Beams with the Atmosphere, Las Cruces, NM, 1/28/86.

"Nonlinear Spectroscopy from Single Micrometer-Size Droplets," Sandia National Laboratories, Livermore, CA, 2/6/86.

"Nonlinear Optics of Microparticles," Korean Advanced Institute of Science and Technology, Seoul, Korea, 2/22/86 and 2/25/86.

"Laser Scattering from Micron-Size Particles," Workshop on Laser Spectroscopy and Techniques, National Central University, Chung-Li, Taiwan, 3/1/86.

"Nonlinear Interaction in Droplets," Academia Sinica, Nankang, Taiwan, 3/3/86.

"Stimulated Oscillations in Micron-Size Objects," National Tsing-Hua University, Hsinchu, Taiwan, 3/5/86.

"High Intensity Laser Interactions with Liquid Droplets," Chung-Shan Institute of Science and Technology, Lung-Tan, Taiwan, 3/7/86.

"Laser Scattering from Micron-Size Particles," Department of Physics, Chinese University of Hong Kong, 4/3/86.

"Nonlinear Optical Interactions from Droplets," Fudan University, Shanghai, People's Republic of China, 4/11/86.

"Laser Interactions with Microparticles," Sichuan University, Cheng Du, People's Republic of China, 4/15/86.

"Nonlinear Optical Interactions in Liquid Droplets during High Intensity Laser Propagation," International Conference on Optical Millimeter Wave Propagation and Scattering in the Atmosphere, Florence, Italy, 5/28/86 (invited talk).

"Droplet Characterization by Light Scattering," International Conference on Optical Millimeter Wave Propagation and Scattering in the Atmosphere, Florence, Italy, 5/30/86 (invited talk).

"Investigation of Superradiant LDV Markers and Three-Component Velocity Mapping," Air Force Office of Scientific Research Workshop on Diagnostics of Reacting Flows, Stanford University, Stanford, CA, 6/17/86.

"Nonlinear Scattering with Droplets," Sanders Associates, Nashua, NH, 7/18/86.

"Nonlinear Optical Diagnostics of Single Droplets," Symposium on HAN-Based Liquid Propellant Flames, Properties, and Structures," Ballistic Research Laboratory, Aberdeen Proving Ground, MD, 7/30/86.

"Lasing and Other Nonlinear Optical Effects from Single Droplets," International Laser Science Conference and the Annual Meeting of the Optical Society of America, Seattle, WA, 10/23/86 (invited talk).

"Laser-Induced Explosion of H_2O Droplets," Workshop on the Interactions of Electromagnetic and Particle Beams with the Atmosphere, Las Cruces, NM, 1/28/87.

"Nonlinear Optical Diagnostics of Diesel Droplets," 15th Meeting of the DOE/Diesel Cooperative Program Working Group, Columbus, IN, 2/5/87.

"Laser Scattering with Individual Liquid Droplets," Physics Colloquium, Wesleyan University, Middletown CT, 2/9/87.

"Nonlinear Optics with Single Droplets," E. I. du Pont de Nemours & Company, Wilmington, DE, 3/20/87.

"Nonlinear Optical Effects of Liquid Droplets," Fifteenth International Quantum Electronics Conference and Conference on Laser and Electro-Optics, Baltimore, MD, 4/30/87 (invited talk).

"Explosive Vaporization of Droplets by Lasers," Mini-Symposium on HAN-Based Liquid Propellant Flames, Properties, and Strucures," Ballistic Research Laboratory, Aberdeen Proving Ground, MD, 5/1/87.

"Nonlinear Optical Phenomena in Single Micron-Size Liquid Droplets," Third USA-USSR Binational Symposium on Laser Optics of Condensed Matter, Leningrad, USSR, 6/3/87 (invited talk).

"High Intensity Visible Laser-Induced Plasma with Transparent Liquid Droplets," 1987 CRDEC Scientific Conference on Obscuration and Aerosol Research, Aberdeen Proving Ground, MD, 6/24/87.

"Laser-Induced Vaporization in Water Droplets," Los Alamos National Laboratory, Los Alamos, NM, 7/8/87.

"Nonlinear Optical Diagnostics of Liquid Droplets," Gordon Research Conference on Laser Diagnostics of Combustion, Plymouth, NH, 7/15/87 (invited talk).

"Laser Scattering from Microparticles," US-Mexico Workshop on Electrodynamics of Interfaces and Composite Systems, Taxco, Mexico, 8/12/87 (invited talk).

"Nonlinear Spectroscopy of Water Droplets Containing Nitrates," Symposium on HAN-Based Liquid Propellant, Flames, and Structures," Ballistic Research Laboratory, Aberdeen Proving Ground, MD, 8/25/87.

"Stimulated Processes in Liquid Droplets," Physics Department, Colorado State University, Fort Collins, CO 9/14/87.

"Nonlinear Optical Scattering from a Single Droplet," American Association for Aerosol Research 1987 Annual Meeting, Seattle, WA, 9/15/87 (invited talk).

"Laser-Induced Breakdown Spectroscopy on Single Transparent Droplets," Physics Department, City College, CUNY, New York, NY, 9/23/87.

"Nonlinear Optical Interaction of Laser Radiation with Water Droplets," Topical Meeting on Laser and Optical Remote Sensing: Instrumentation and Techniques, North Falmouth, MA, 10/1/87 (invited talk).

"Nonlinear Optical Spectroscopy of Liquid Droplets: Chemical Composition within the Interface," ARO 7th Engine/Fuels Workshop, Detroit, MI, 10/14/87.

"Status Report on Laser-Induced Breakdown in Single Droplets," ARO Workshop on Laser Propagation and Scattering in the Atmosphere, Rochester, NY, 10/23/87.

"Photon Lifetime within a Droplet," IBM Research Center, Yorktown Heights, NY, 11/30/87.

"Lasing and Other Stimulated Scattering Processes in Single Droplets," Lasers '87, Lake Tahoe, NV, 12/10/87 (invited talk).

"Laser-Induced Breakdown in Solid Particles," Aerospace Corp., El Segundo, CA, 12/17/87.

Marshall B. Long:

"Simultaneous Temperature and Species Mapping in Turbulent Nonpremixed Flames," Fifth Meeting of the Sandia Cooperative Group on the Aerthermochemistry of Turbulent Combustion, University of California at San Diego, 4/1/85.

"Advanced Laser Imaging Techniques in Turbulent Flows," University of California at Irvine, 6/27/85.

"Two-Dimensional Imaging," Gordon Research Conference on Physics and Chemistry of Laser Diagnostics in Combustion, 7/18/85.

"Instantaneous Two-Dimensional Mapping of the Complete Three-Dimensional Scalar Gradient," Sandia Cooperative Group, Cornell University, 10/8/85.

"Laser Diagnostics in Turbulent Reacting and Nonreacting Flows," University of Montana, 10/10/85.

"Quantitative Imaging in Turbulent Flames: Measurements in Two Dimensions and Beyond," Carnegie-Mellon, Pittsburgh, PA, 11/13/85.

"Imaging in Turbulent Flames: Measurements in Two Dimensions and Beyond," General Motors Research Laboratories, Detroit, MI, 2/6/86.

"Laser Diagnostics in Turbulent Reacting and Nonreacting Flows," University of Dayton, 2/21/86.

"Imaging System Requirements for Turbulence and Combustion Diagnostics," Topical Meeting on Quantum Limited Imaging and Image Processing," Honolulu, HI 3/31/86.

"Imaging in Turbulent Flames: Measurements in Two Dimensions and Beyond," Ford Motor Company, Dearborn, MI, 4/29/86.

"Imaging in Turbulent Flames: Measurements in Two Dimensions and Beyond," IBM Research Center, San Jose, CA, 6/10/86.

"Quantitative Imaging Techniques for Turbulence and Combustion Diagnostics," Conference on Lasers and Electro-Optics (CLEO'86), San Francisco, CA, 6/13/86 (invited talk).

"Investigation of Superradiant LDV Markers and Three-Component Velocity Mapping," AFOSR Contractors Meeting on Diagnostics of Reacting Flows, Stanford University, Stanford, CA, 6/17/86.

"Laser Diagnostics Beyond Two Dimensions," International Laser Science Conference, Seattle, WA, 10/24/86 (invited talk).

"Three-Dimensional Measurements in Gas Flows," International Congress on the Applications of Lasers and Electro-Optics (ICALEO '86), Arlington, VA, 11/11/86.

"Imaging in Turbulent Flames: Measurements in Two-Dimensions and Beyond," Princeton University, Princeton, NJ, 11/14/86.

"Simultaneous Multipoint Measurements of Density Gradients and Temperature in a Flame," California Institute of Technology, Pasadena, CA, 2/4/87.

"Imaging in Turbulent Flows and Flames: Measurements in Two-Dimensions and Beyond":
University of Tokyo, Tokyo, Japan, 2/21/87.
Japan National Aerospace Laboratory, Tokyo, Japan, 2/24/87.
Mechanical Engineering Laboratory of the Ministry of International Trade and Industry, Ibaraki-ken, Japan, 2/25/87.
Kyoto University, Kyoto, Japan, 2/27/87.
Kobe University, Kobe, Japan, 3/2/87.
Mitsubishi Electric, Itami City, Japan, 3/5/87.
Nagoya University, Nagoya, Japan, 3/6/87.
Toyota Central Research and Development Laboratories, Aichi, Japan, 3/9/87.
Keio University, Tokyo, Japan, 3/12/87.
Tokyo Institute of Technology, Tokyo, Japan, 3/13/87.
National Tsing Hua University, Hsinchu, Taiwan, 3/18/87.
Academia Sinica, Taipei, Taiwan, 3/20/87.
National Central University, Chung Li, Taiwan, 3/23/87.
Chung Shan Institute of Science and Technology, Chung Chan, Taiwan, 3/24/87.
National Chiao Tung University, Hsinchu, Taiwan, 3/26/87.
Ruhr-Universitat, Bochum, West Germany, 4/87.
Cambridge University, Cambridge, England, 5/87.
Imperial College of Science and Technology, London, England, 5/87.
Cambridge University, Cambridge, England, 5/87.

"Advances in Imaging Techniques for Two and Three-Dimensional Measurements," Gordon Research Conference on Physics and Chemistry of Laser Diagnostics in Combustion, Plymouth, NH, 7/13/87 (invited talk).

"Measurement of the Topology of Large-Scale Structures in Turbulent Reacting Flow," U.S.-France Workshop on Turbulent Reactive Flows, Rouen, France, 7/7/87 (invited talk).

"Laser Rayleigh Imaging in Turbulent Premixed Flames," Tenth Meeting of the Sandia Cooperative Group on Turbulent Combustion, General Motors Research Laboratories, Warren, MI, 10/12/87.

"Advances in Electronic Imaging," International Congress on the Applications of Lasers and Electro-Optics (ICALEO '87), San Diego, CA, 11/8/87 (invited talk).

INTERACTIONS WITH OTHER LABORATORIES

Richard K. Chang:

CRDEC, Aberdeen Proving Ground, MD
Dr. J. White, Dr. J. Embury and Dr. I. Sindoni

U.S. Army Sciences Laboratory, White Sands Missile Base, NM
Dr. R. Pinnick and Dr. D. Pendleton

Ballistic Research Laboraties, Edgewood, MD
Dr. A. Miziolek and Dr. N. Klein

Sandia National Laboratories, Livermore CA
Dr. Peter Mattern and Dr. Billie Sanders

Marshall B. Long:

United Technologies Research Center, East Hartford, CT
Dr. Alan Eckbreth and Dr. Alexander Vranos

General Electric Research Laboratory, Schenectady, NY
Dr. Sanjay Correa

Sandia National Laboratories, Livermore, CA
Dr. Sheridan Johnston and Dr. Robert Dibble

END

DATE

FILMED

8-88

DTIC